

## UPWARD CONTINUATION OF DOME-C AIRBORNE GRAVITY AND COMPARISON TO GOCE GRADIENTS AT ORBIT ALTITUDE IN EAST ANTARCTICA

Hasan Yildiz<sup>1\*</sup>, Rene Forsberg<sup>2</sup>, C. Christian Tscherning deceased<sup>3</sup>, Daniel Steinhage<sup>4</sup>, Graeme Eagles<sup>4</sup>, Johannes Bouman<sup>5</sup>

1. Geodesy Department, General Command of Mapping, Ankara, Turkey.
2. DTU-Space, Denmark Technical University, Copenhagen, Denmark
3. Niels Bohr Institute (NBI), University of Copenhagen, Denmark
4. Alfred Wegener Institute (AWI) Helmholtz Centre for Polar and Marine Research, Bremerhaven, Germany
5. Deutsches Geodätisches Forschungsinstitut der Technischen Universität München (DGFI-TUM), Arcisstrasse 21, 80333 Munich, Germany

An airborne gravity campaign was carried out at the Dome-C survey area in East Antarctica between the 17th and 22nd of January 2013, in order to provide data for an experiment to validate GOCE satellite gravity gradients. After typical filtering for airborne gravity data, the cross-over error statistics for the few crossing points are 11.3 mGal r.m.s., corresponding to an r.m.s. line error of 8.0 mGal. This number is relatively large due to the rough flight conditions, short lines and field handling procedures used. Comparison of the airborne gravity data with GOCE RL4 spherical harmonic models, confirmed the quality of the airborne data and that they contain more high frequency signal than the global models. First, the airborne gravity data were upward continued to GOCE altitude to predict gravity gradients in the local North-East-Up reference frame applying least squares collocation using the ITG-GRACE2010S field to degree and order 90 as reference field, which is subtracted from both the airborne gravity and GOCE gravity gradients. Then, the predicted gradients are rotated to the **gradiometer reference frame** using **level 1** attitude quaternion

---

\* The manuscript solely reflects the personal views of the author and does not necessarily represent the views, positions, strategies or opinions of Turkish Armed Forces.

1  
2  
3 data. The validation with the airborne gravity data is limited to the accurate gradient anomalies  
4  
5 ( $T_{XX}$ ,  $T_{YY}$ ,  $T_{ZZ}$  and  $T_{XZ}$ ) where the long-wavelength information of the GOCE gradients has been  
6  
7 replaced with GOCO03s signal to avoid contamination with GOCE gradient errors at these  
8  
9 wavelengths. The comparison shows standard deviations between the predicted and GOCE gradient  
10  
11 anomalies of 9.9 mE, 11.5 mE, 11.6 mE and 10.4 mE ( $T_{XX}$ ,  $T_{YY}$ ,  $T_{ZZ}$  and  $T_{XZ}$ ). A more precise  
12  
13 airborne gravity survey of the southern polar gap which is not observed by GOCE would thus  
14  
15 provide gradient predictions at a better accuracy, complementing the GOCE coverage in this region.  
16  
17

## 18 19 20 21 **1. INTRODUCTION** 22 23 24

25 An airborne survey (Dome-C) was carried out around Antarctica's Dome-C/Concordia station on  
26  
27 17-22 January 2013. The Dome-C survey aimed to collect radiometric and gravity data for  
28  
29 calibration and validation of measurements made by the Soil Moisture and Ocean Salinity (SMOS)  
30  
31 (Mecklenburg et al., 2012) and Gravity Field and Steady-state Ocean Circulation Explorer (GOCE)  
32  
33 (ESA, 1999) satellites, two European Space Agency (ESA) Earth Explorer missions. The  
34  
35 investigation was limited to a 300 km by 300 km area around the wintering station Concordia on  
36  
37 Dome-C in East Antarctica (Fig.1). Field operations for both the radiometer and airborne gravity  
38  
39 measurements are described in detail by Steinhage et al. (2013). Validation of the SMOS data is  
40  
41 reported by Kristensen et al. (2013). By comparison to the Dome-C aerogravity data, this study  
42  
43 aims to compare the upward continued airborne gravity data with GOCE gradients in the  
44  
45 gradiometer reference frame (GRF) at satellite altitude. If this can be demonstrated to give  
46  
47 satisfactory results, upward continuation of airborne gravity survey data proposed by Forsberg et al.  
48  
49 (2011) could be an efficient solution to the Antarctic polar gap problem in GOCE (Rudolph et al.,  
50  
51 2002; Tscherning et al., 2000).  
52  
53  
54  
55  
56  
57  
58  
59  
60

1  
2  
3 Different methods and concepts have been suggested for the external validation of satellite gravity  
4  
5 gradients. Validation with gravity field models are used in Visser et al. (2000), Bouman et al.  
6  
7 (2004) and Bouman and Fuchs (2012). Numerical integration approach with truncated kernels using  
8  
9 ground gravity data was suggested by Haagmans et al. (2003), Denker (2003), Pail (2003), Kern  
10  
11 and Haagmans (2005), Wolf and Denker (2005). Eshagh (2009 and 2010) proposed the use of least-  
12  
13 squares modified integral formulas for transformation of ground gravity onto satellite gravitational  
14  
15 gradients. Eshagh (2011a) suggested validation of the radial gravitational gradient by the geoid  
16  
17 undulation using semi-stochastic modifications of the Abel-Poisson integral equation. Šprlák et al.  
18  
19 (2015), extending the study of Eshagh (2011a), presented new integral equations for all six  
20  
21 components of the gradiometric tensor at satellite altitude and validated the GOCE vertical gravity  
22  
23 gradient using satellite altimetry data at 11 mE level. Least squares collocation with ground gravity  
24  
25 data was used for the same purpose by Arabelos and Tscherning (1998), Wolf and Denker (2005),  
26  
27 Arabelos et al. (2007) and Pail (2003). Zielinsky and Petrovskaya (2003) suggested the use of  
28  
29 gravitational gradients measured by a balloon-borne gradiometer whereas Tóth et al. (2005)  
30  
31 suggested the use of terrestrial torsion balance observations to validate satellite gravitational  
32  
33 gradients.

34  
35  
36  
37  
38  
39  
40 On the other hand, the least squares collocation method was applied to satellite gravitational  
41  
42 gradients for regional gravity field recovery by Schwarz and Krynski (1977), Arabelos and  
43  
44 Tscherning (1990), Barzaghi et al. (2009), Yildiz (2012) and Herceg et al. (2015). Implementation  
45  
46 of integral formulas to satellite gravitational gradients for regional gravity field recovery were  
47  
48 proposed by van Gelderen and Rummel (2001), Tóth et al. (2002), Martinec (2003), Bölling and  
49  
50 Grafarend (2005), Eshagh (2011b). Radial base functions were used by Eicker et al. (2014) and  
51  
52  
53  
54  
55  
56  
57  
58  
59  
60

1  
2  
3 Lieb et al. (2014) whereas multi-scale approach was used by Freeden et al. (2002), Freeden and  
4  
5 Nutz (2011) for regional gravity field recovery using satellite gravitational gradients.  
6  
7

8  
9  
10 This manuscript firstly describes the Dome-C airborne gravity data collection and comparison to  
11  
12 GOCE spherical harmonic models and consequently focuses on the upward continuation of  
13  
14 Dome-C airborne gravity to observed GOCE gradients in the GRF at orbital altitude using the LSC  
15  
16 method.  
17

## 20 21 **2. AIRBORNE GRAVITY: THE DOME-C SURVEY**

22  
23

24  
25 The gravity measurements at Dome-C were carried out on all the main lines of the regular planned  
26  
27 flight pattern, as well as a few cross lines and opportunistic flights. The gravity measurements were  
28  
29 made using the Alfred Wegener Institute's (AWI) Lacoste and Romberg S-56 gravimeter, upgraded  
30  
31 by Zero-Length Spring (ZLS) corporation for airborne data collection. This kind of instrumentation  
32  
33 is common in airborne surveys worldwide, including in Antarctica (e.g. Forsberg et al., 2011;  
34  
35 Riedel et al., 2012). The basic principle of the instrument is a servo-feedback spring system on a  
36  
37 gyro stabilized table. To obtain sufficiently accurate results it is essential to understand and model  
38  
39 the numerous potential errors in the system, especially scale factors and platform off-level errors.  
40  
41 For more details of airborne gravity measurement principles and corrections see e.g. Olesen (2002)  
42  
43 and Forsberg and Olesen (2010).  
44  
45  
46  
47

48  
49 The airborne gravity survey at Dome-C took place in the period 17-22 January 2013, with gravity  
50  
51 additionally collected on the ferry flights to Dome-C from Novolazarevskaya via South Pole. The  
52  
53 list of the survey flights for the Dome-C air campaign can be found in Steinhage et al. (2013).  
54  
55  
56  
57  
58  
59  
60

1  
2  
3  
4  
5 As gravity cannot be measured during aircraft turns, and filters are needed to settle the  
6  
7 measurements after turns, only parts of the longer lines could be processed to give useful gravity  
8  
9 data, cf. Fig. 2. The airborne gravity processing was done at AWI, using software originally based  
10  
11 on code from Olesen (2002), and further modified over a number of years by U. Meyer,  
12  
13 Bundesanstalt für Geowissenschaften und Rohstoffe (BGR)-Germany and AWI. The measurements  
14  
15 were tied to an absolute International Gravity Standardization Net (IGSN) gravity reference point at  
16  
17 University of Cape Town: reference value 979616.80 mGal. Then, the measurements were  
18  
19 transferred to Novo runway, Amundsen-Scott South Pole Station and Dome-C, using measurements  
20  
21 with a portable Lacoste and Romberg land gravity meter (serial number G744). A recent absolute  $g$ -  
22  
23 value measured by Finnish Geodetic Institute at Novolazerevskaya in Antarctica (Fig. 1) has been  
24  
25 used for a final adjusted value for the Dome-C reference gravity  $g=981861.29$  mGal. The revised  
26  
27 value was used in this manuscript. GPS positions, velocities and accelerations were computed with  
28  
29 the commercial “Waypoint” software package “GrafNav” (NovAtel Inc.  
30  
31 Calgary, Canada), which is state-of-the art kinematic GPS software allowing both differential phase  
32  
33 and precise point positioning techniques to be used with the highest precision. Filtering used in the  
34  
35 processing was a 3-stage forward-backward Butterworth filtering with time constant 20 s, and  
36  
37 clipping 200 s, a typical set up for airborne gravimetry.  
38  
39  
40  
41  
42  
43  
44

45 The airborne gravity data was processed without use of geoid heights, and the anomalies are  
46  
47 therefore to be considered as gravity disturbances (Fig. 2). The gravity disturbances were converted  
48  
49 to free-air gravity anomalies using geoid values from GOCE RL4 “direct” spherical harmonic  
50  
51 model (Bruinsma et al., 2013). The conversion from gravity disturbances to gravity anomalies is a  
52  
53 geodetic convention, in line with common global practice for airborne gravimetry; with the GOCE  
54  
55  
56  
57  
58  
59  
60

geoid being accurate at the 0.5 m level or better, the associated error in applying the geoid correction is less than 0.2 mGal and thus negligible, compared to the accuracy of the airborne data.

The cross-over error statistics of the free-air gravity anomalies for the few cross-lines are shown in Fig. 3, indicating a relatively noisy survey of 12.8 mGal r.m.s. error for 22 line crossings. Eliminating two very large outliers, the survey cross-over error is at 11.3 mGal r.m.s., corresponding to an r.m.s. line error of 8.0 mGal. This number is relatively large due to the rough flight conditions, short lines and field handling procedures used.

### 3. UPWARD CONTINUATION AND COMPARISON TO OBSERVED GOCE DATA

#### a. Methodology

The airborne gravity data were compared with GOCE RL4 “direct” spherical harmonic model data, and upward continuation was done to GOCE orbit altitude. This processing was done with the GRAVSOFIT suite of programs (Tscherning et al, 1992; Forsberg and Tscherning, 2008), implementing the upward continuation using LSC method.

In the LSC method the upward continuation to gravity gradients is performed by solving a set of equations, of dimensions equal to the number of data

$$\hat{s} = C_{sx} [C_{xx} + D]^{-1} x \quad (1)$$

where the signal  $s$  is the desired set of gradient components,  $x$  are the airborne gravity observations, and  $C_{sx}$  and  $C_{xx}$  the cross- and auto-covariances of the gravity field components, derived from a self-consistent covariance model, and  $D$  the errors. For details see Heiskanen and Moritz (1967). The

LSC method is implemented by the latest version of GRAVSOFT's GEOCOL program, GEOCOL19, using multi-processing (Kaas et al., 2013).

For the least squares collocation computation a spherical harmonic reference field

$$T_{ITG2010S}(r, \varphi, \lambda) = \frac{GM}{R} \sum_{n=2}^{90} \left(\frac{R}{r}\right)^{n+1} \sum_{m=0}^n (C_{nm} \cos m\lambda + S_{nm} \sin m\lambda) P_{nm}(\sin \phi) \quad (2)$$

is used in a remove-restore fashion, where  $r, \varphi, \lambda$  are spherical geocentric coordinates of the computation point (radius, latitude, longitude),  $R$  is the mean semi-major axis of the Earth,  $GM$  is the gravitational constant times mass of the Earth,  $n$  and  $m$  are spherical harmonic degree and order, respectively,  $P_{nm}$  are fully normalized Legendre functions and  $C_{nm}, S_{nm}$  are fully normalized Stokes' coefficients.

In the Dome-C computations we have used the ITG-GRACE2010S field to degree and order 90 as the fundamental reference field. The degree 90 reference field corresponds to a spherical harmonic resolution of  $2^\circ$ , smaller than the size of the Dome-C survey area. It is also a spherical harmonic range in which the accuracy of ITG-GRACE2010S is very good, being determined by GRACE data and therefore independent of GOCE.

### b. Data and Covariance Function Computation

The AWI-processed airborne gravity data were compared to the GOCE "direct" RL4 model, after corrections removing the effects of the atmosphere (approx. +0.6 mGal), and adjustment of the

1  
2  
3 gravity tie measurements provided by AWI in the light of the new absolute measurements at  
4  
5 Novolazarevskaya. The estimated error in the adjusted  $g$  value at Dome-C is 0.2 mGal. Using this  
6  
7 value, the AWI data were corrected for the atmosphere and geoid undulations, using the GOCE  
8  
9 direct RL4 model, giving the final free-air anomaly data set, used for all computations in the  
10  
11 following.  
12

13  
14  
15  
16 Statistical comparisons of the AWI airborne free air gravity anomaly data to the GOCE RL4  
17  
18 “direct” and “timewise” models (Pail et al., 2011), as a function of maximal degree, are shown in  
19  
20 Table 1. The comparison in Table 1 shows that the standard deviation of the difference seems to  
21  
22 decrease consistently with the higher cut-off in the RL4 fields, all the way to the maximal degree  
23  
24 (260 or 250). The small bias of  $\sim 1$  mGal is likely due to the limited size of the comparison region.  
25  
26 Fig. 4 shows the airborne and GOCE gravity anomalies obtained from GOCE RL4 “direct” model  
27  
28 to degree 200.  
29  
30

31  
32  
33  
34 GOCE observed the six gravitational gradients in the GRF that co-rotates with the satellite, where  
35  
36 the  $V_{XX}$ ,  $V_{YY}$ ,  $V_{ZZ}$  and  $V_{XZ}$  gradients have been observed with high accuracy in a measurement  
37  
38 band (MB) that roughly corresponds to a spatial resolution of 80 – 1500 km, and error increase  
39  
40 above and below the MB (Bouman et al., 2011a). One could transform the measured gradients into  
41  
42 the local North-East-Up reference frame using model values for the less accurate  $V_{XY}$  and  $V_{YZ}$   
43  
44 components and replacing the GOCE gradient signal below the MB with model values also for the  
45  
46 accurate gradients, circumventing the affection through the GOCE gradient long wavelength errors  
47  
48 (Fuchs and Bouman, 2011). However, this inherently introduces a mixture in the MB of measured  
49  
50 and model gradients in the local North-East-Up reference frame, which may be undesirable. For the  
51  
52 GOCE validation, it is therefore preferable to do the validation directly in the GRF, rather than the  
53  
54  
55  
56  
57  
58  
59  
60



1  
2  
3 local North-East-Up reference frame. A persisting problem of the GOCE gradients in the GRF,  
4  
5 however, is the error increase above and below the MB. We therefore used band-pass filtered  
6  
7 gravity gradients, replacing the signal below the MB with signal derived from GOCO03s model  
8  
9 (Mayer-Gürr et al., 2012), where the model gradients were filtered with the complement of the  
10  
11 band-pass filter to guarantee that the sum of the band-pass filtered GOCE and low-pass filtered  
12  
13 model gradients contains the full signal content. The cut-off frequency of 10 mHz in the lower MB  
14  
15 roughly corresponds to spherical harmonic degree 54. In other words, GOCO03s has little or no  
16  
17 contribution above degree 54, whereas the GOCE gradients do not contribute below degree 54.  
18  
19 Because we subtract the reference model ITG-GRACE2010S up to degree 90 from the GOCE-  
20  
21 based gradients and because GOCO03s mainly contains GRACE information for low degrees, it is  
22  
23 reasonable to assume that the error of the reduced GOCE-based gradients mainly reflects the error  
24  
25 of the original GOCE gradients in the MB above 10 mHz.  
26  
27  
28  
29  
30

31 GOCE gravity gradients – combined with GOCO03s for the long wavelengths – were selected in a  
32  
33 central region (76-73°S, 113-126° E) for the year 2011, yielding  $4 \times 19208$  data points in total.  
34  
35 From the GOCE-based GRF gravity gradient data the ITG-GRACE2010S contribution up to degree  
36  
37 90 was subtracted and gradient anomalies ( $T_{XX}$ ,  $T_{YY}$ ,  $T_{ZZ}$  and  $T_{XZ}$ ) are obtained.  
38  
39  
40  
41

42 The prediction of gravity gradient anomalies in the local North-East-Up reference frame from the  
43  
44 airborne gravity anomalies has been done using the LSC method described in Tscherning (1993), as  
45  
46 implemented in the **GEOCOL19** program. First, gravity gradient anomalies are predicted in the  
47  
48 GOCE orbit points in the local North-East-Up reference frame. Next the predicted gradients are  
49  
50 rotated to the GRF using as input the **level 1** attitude quaternion data that define the transformation  
51  
52 between the inertial reference frame and the GRF, as well as **level 2** precise orbit information that  
53  
54  
55  
56  
57  
58  
59  
60

1  
2  
3 allows to derived the transformation from the inertial reference frame to the local North-East-Up  
4  
5 reference frame (Gruber et al., 2010). Subsequently, the upward continued gravity gradient anomaly  
6  
7 data from the airborne survey were compared to the GOCE gradient anomalies.  
8  
9

10  
11 Airborne free air gravity anomaly data of 6444 points were selected (pixel binning to approximately  
12  
13 2 km resolution), to which an empirical, self-consistent covariance function of the Tscherning and  
14  
15 Rapp (1974) type was fitted. Fig. 5 shows the estimated and fitted covariance model, which  
16  
17 represents a typical data covariance function (after subtraction of the ITG-GRACE2010S up to  
18  
19 degree 90 reference field), with the depth to the Bjerhammar sphere of 5.1 km. This covariance  
20  
21 function has been used to predict gravity gradient anomaly errors at altitude in the local North-East-  
22  
23 Up reference frame, using the GRAVSOF program GEOCOL19 taking the standard error of the  
24  
25 airborne gravity anomaly as 8 mGal to investigate the error propagation of the airborne gravity  
26  
27 survey to the estimated gravity gradients. We obtained estimated gradient anomaly errors of 5.9  
28  
29 mE, 5.5 mE, 8.0 mE and 6.8 mE for  $T_{XX}$ ,  $T_{YY}$ ,  $T_{ZZ}$  and  $T_{XZ}$  at altitude in the local North-East-Up  
30  
31 reference frame, respectively, showing that the available airborne gravity data can validate the  
32  
33 GOCE gradients, considering that the expected noise of GOCE gravitational gradients for short time  
34  
35 intervals is about 10 mE (Bouman et al. 2011b; Šprlák et al. 2015).  
36  
37  
38  
39  
40  
41  
42

43 Subsequently, we assumed a standard error in the airborne gravity anomaly of 3 mGal r.m.s. (this  
44  
45 avoids filtering surface data too heavily, and partially takes into account the surface data selection  
46  
47 process) to predict gravity gradient anomalies and their errors at altitude in the local North-East-Up  
48  
49 reference frame. These were then rotated to the GRF to compare with GOCE gradients in the next  
50  
51 section.  
52  
53  
54  
55  
56  
57  
58  
59  
60

### c. Comparison of observed and predicted GOCE gravity gradients

Figures 6 shows the predicted GOCE gradients (minus the reference field) by LSC, and Figure 7 shows the difference between GOCE observations and upward continued values for ascending and descending tracks. As the gravity gradients have directional sensitivity and especially the GRF X-axis and Y-axis have a different orientation for ascending and descending tracks,  $T_{XX}$ ,  $T_{YY}$  and  $T_{XZ}$  are plotted separately for ascending and descending tracks. Partially the differences are spatially correlated, which may be caused by remaining long wavelength errors in the airborne or GOCE data or both. In addition, some satellite tracks show larger differences that may be caused by unflagged erroneous GOCE data, e.g., after filter re-initialization.

Table 2 shows the statistics of the comparison of gradient anomalies. This comparison shows standard deviations, between the predicted and GOCE gradient anomalies of 9.9 mE, 11.5 mE, 11.6 mE and 10.4 mE in the gradient anomalies  $T_{XX}$ ,  $T_{YY}$ ,  $T_{ZZ}$  and  $T_{XZ}$  respectively, thus validating GOCE measurements in agreement with the expected noise of GOCE gravitational gradients which is about 10 mE (Bouman et al.,2011b; Šprlák et al.,2015).

## 4. CONCLUSION

The Dome-C gravity survey successfully covered a hitherto unsurveyed and logistically very difficult region of Antarctica. The survey provided a consistent gravity data set with a reasonably small bias of 1 mGal compared to GOCE, and an estimated track r.m.s. noise of 8 mGal. We believe that the bias is primarily due to the small size of the survey area, as airborne gravity is usually biased by less than 1 mGal (Forsberg and Olesen, 2010).

1  
2  
3  
4  
5 The airborne gravity data agrees with the GOCE data with ~14 mGal r.m.s. difference; results for  
6  
7 the “direct” and “timewise” R4 spherical harmonic models are nearly identical. This difference is  
8  
9 mainly due to the omission error that has its origin in the limited resolution of GOCE. The  
10  
11 comparison for various spherical harmonic degrees shows that the GOCE data provide an  
12  
13 improving r.m.s. fit to the airborne data with increasing degree of the maximal spherical harmonic  
14  
15 expansion, all the way to the maximal degree (250 for timewise, and 260 for direct).  
16  
17

18  
19  
20 Collocation upward continuation of the airborne gravity anomaly data to gravity gradient anomalies  
21  
22 in the North-East-Up reference frame and transformation to GRF at orbital altitude were carried out  
23  
24 for the accurate gradient anomalies ( $T_{XX}$ ,  $T_{YY}$ ,  $T_{ZZ}$ ,  $T_{XZ}$ ), using quaternions of the GOCE level 1  
25  
26 data. This comparison shows a common error of ~10 mE for gradient anomalies ( $T_{XX}$ ,  $T_{YY}$ ,  $T_{ZZ}$ ,  
27  
28  $T_{XZ}$ ) thus validating GOCE gradients at this level.  
29  
30  
31

32  
33  
34 A more precise airborne gravity survey of the southern polar gap as proposed by Forsberg et al.  
35  
36 (2011) would thus be expected to provide gradient predictions at a better accuracy, complementing  
37  
38 the coverage of GOCE in this region.  
39  
40  
41

#### 42 **Acknowledgements**

43  
44 All computations for the gravity field transformations in this manuscript were done using the DTU-  
45  
46 Space GRAVSOFT package. We additionally thank Jaakko Makinen, Finnish Geodetic Institute,  
47  
48 for providing the absolute gravity value at Novo station.  
49  
50  
51  
52  
53  
54  
55  
56  
57  
58  
59  
60

**REFERENCES**

Arabelos D, Tscherning CC (1990) Simulation of regional gravity field recovery from satellite gravity gradiometer data using collocation and FFT. *Journal of Geodesy* 64: 363-382.

Arabelos D, Tscherning CC (1998) Calibration of satellite gradiometer data aided by ground gravity data. *Journal of Geodesy* 72: 617–625.

Arabelos D, Tscherning CC, Veichert M (2007) External calibration of GOCE SGG data with terrestrial gravity data: a simulation study. In: Tregoning P, Rizos C (eds) *Dynamic planet*, IAG Symposia Series, vol. 130, Springer, 337–344.

Barzaghi R, Tselfes N, Tziavos IN, Vergos GS (2009) Geoid and high resolution topography modelling in the Mediterranean from gravimetry, altimetry and GOCE data: evaluation by simulation. *Journal of Geodesy*, 83, 751-772.

Bölling C, Grafarend EW (2005) Ellipsoidal spectral properties of the Earth's gravitational potential and its first and second derivatives. *Journal of Geodesy* 79: 300-330.

Bouman J, Koop R, Tscherning CC, Visser P (2004) Calibration of GOCE SGG data using high-low SST, terrestrial gravity data and global gravity field models. *Journal of Geodesy*, 78, 124-137.

Bouman J, Fiorot S, Fuchs M, Gruber T, Schrama E, Tscherning CC, Veichert M, Visser P (2011a) GOCE Gravity Gradients along the Orbit, *Journal of Geodesy*, 85: 791-805, DOI: 10.1007/s00190-011-0464-0.

Bouman J, Bosch W, Sebera J (2011b) Assessment of systematic errors in the computation of gravity gradients from satellite altimetry. *Marine Geodesy* 34: 85–107.

1  
2  
3 Bouman J, Fuchs M (2012) GOCE gravity gradients versus global gravity field models.  
4  
5 Geophysical Journal International, 189: 846-850.  
6

7  
8 Bruinsma S, Förste C, Abrikosov O, Marty JC, Rio M-H, Mulet S, Bonvalot S (2013) The new ESA  
9  
10 satellite-only gravity field model via the direct approach, Geophysical Research Letters, 40, 14,  
11  
12 3607-3612. DOI: 10.1002/grl.50716.  
13  
14

15  
16 Denker H (2003) Computation of gravity gradients for Europe for calibration/validation of GOCE  
17  
18 data. In: Tziavos IN (ed) Gravity and Geoid 2002, 3rd Meeting of the IGGC, Ziti Editions, 287–  
19  
20 292.  
21  
22

23  
24 Eicker A, Schall J, Kusche J (2014) Regional gravity modelling from spaceborne data: case studies  
25  
26 with GOCE. Geophysical Journal International 196: 1431-1440.  
27  
28

29  
30 ESA (1999) Gravity field and steady-state ocean circulation mission, Reports for mission selection;  
31  
32 the four candidate Earth explorer missions, SP-1233(1), European Space Agency.  
33  
34

35  
36 Eshagh M (2009) Towards validation of satellite gradiometric data using modified version of 2nd  
37  
38 order partial derivatives of extended Stokes' formula. Artificial Satellites 44: 103–129.  
39  
40

41  
42 Eshagh M (2010) Least-squares modification of extended Stokes' formula and its second-order  
43  
44 radial derivative for validation of satellite gravity gradiometry data. Journal of Geodynamics 49:  
45  
46 92–104.  
47  
48

49  
50 Eshagh M (2011a) Semi-stochastic modification of second-order radial derivative of Abel-Poisson's  
51  
52 formula for validating satellite gravity gradiometry data. Advances in Space Research 47: 757–767.  
53  
54  
55  
56  
57  
58  
59  
60

1  
2  
3 Eshagh M (2011b) On integral approach to regional gravity field modelling from satellite  
4  
5 gradiometric data. *Acta Geophysica* 59:29-54.  
6  
7

8  
9 Forsberg R, Olesen AV, Yildiz H, Tscherning CC (2011) Polar Gravity Fields from GOCE and  
10  
11 Airborne Gravity, Proc. of 4th International GOCE User Workshop, Munich, Germany 31 March –  
12  
13 1 April 2011 (ESA SP-696, July 2011).  
14

15  
16 Forsberg R, Olesen AV(2010) Airborne gravity field determination. In: Xu G (ed): *Sciences of*  
17  
18 *Geodesy – I, Advances ,and Future Directions*, pp. 83-104, Springer Verlag, ISBN 978-3-642-  
19  
20 11741-1.  
21

22  
23  
24 Forsberg R, Tscherning CC (2008) An overview manual for the GRAVSOFTE Geodetic Gravity  
25  
26 Field Modelling Programs. Danish Space Center Technical Report.  
27

28  
29  
30 Freeden W, Volker M, Nutz H (2002) Satellite-to-satellite tracking and satellite gravity gradiometry  
31  
32 (Advanced techniques for high-resolution geopotential field determination). *Journal of Engineering*  
33  
34 *Mathematics* 43: 19-56.  
35

36  
37  
38 Freeden W, Nutz H (2011) Satellite gravity gradiometry as tensorial inverse problem. *International*  
39  
40 *Journal on Geomathematics* 2: 177-218.  
41

42  
43 Fuchs MJ, Bouman J (2011) Rotation of GOCE gravity gradients to local frames, *Geophysical*  
44  
45 *Journal International*, 187: 743–753, DOI: 10.1111/j.1365-246X.2011.05162.x.  
46  
47

48  
49  
50 Gruber T, Rummel R, Abrikosov O, van Hees R (2010) GOCE Level 2 Product Data Handbook,  
51  
52 GO-MA-HPF-GS-0110, Issue 4, Revision 3, [https://earth.esa.int/web/guest/-/goce-level-2-product-](https://earth.esa.int/web/guest/-/goce-level-2-product-data-handbook-pdf-5708)  
53  
54 [data-handbook-pdf-5708](https://earth.esa.int/web/guest/-/goce-level-2-product-data-handbook-pdf-5708).  
55  
56

1  
2  
3 Haagmans R, Prijatna K, Omang OCD (2003) An alternative concept for validation of GOCE  
4 gradiometry results based on regional gravity. In: Tziavos IN (Ed.) Gravity and Geoid 2002, 3rd  
5 Meeting of the IGGC, Ziti Editions, 281–286.  
6  
7  
8

9  
10 Herceg, M., Knudsen, P., Tscherning, C.C. (2015) GOCE Data for Local Geoid Enhancement. In:  
11 Marti, U (Ed.) Gravity, Geoid and Height Systems, Springer, 133-142.  
12  
13  
14

15  
16 Heiskanen W, Moritz H (1967) Physical geodesy. Freeman Publishing.  
17

18  
19 Kaas E, Sørensen B, Tscherning CC, Veicherts M (2013) Multi-Processing least squares  
20 collocation: Applications to gravity field analysis, Journal of Geodetic Science, 3, 219–223,  
21 DOI: 10.2478/jogs-2013-0025.  
22  
23  
24

25  
26 Kern M, Haagmans R (2005) Determination of gravity gradients from terrestrial gravity data for  
27 calibration and validation of gradiometric data. In: Jekeli C, Bastos L, Fernandes L (eds) Gravity,  
28 Geoid and Space Missions, IAG Symposia Series, vol. 129, Springer, 95–100.  
29  
30  
31

32  
33 Kristensen SS, Søbjerg S, Balling J, Skou N (2013) DOMEair Campaign EMIRAD Data:  
34 Presentation & Analysis, Report submitted to ESA, (dated Nov 12, 2013).  
35  
36  
37

38  
39 Lieb V, Bouman J, Dettmering D, Fuchs M, Schmidt M (2014) Combination of GOCE gravity  
40 gradients in regional gravity field modelling using radial basis functions. In: Sneeuw N (Ed.)  
41 Proceedings of the 8th Hotine-Marussi Symposium, Rome, Italy, June 17-21, 2013, IAG Symposia,  
42 Vol. 142,1-8, Springer-Verlag, Berlin.  
43  
44  
45  
46  
47  
48

49  
50 Martinec Z (2003) Green's function solution to spherical gradiometric boundary-value problems.  
51 Journal of Geodesy 77: 41-49.  
52  
53  
54  
55  
56  
57  
58  
59  
60



1  
2  
3 Mayer-Gürr T, Rieser D, Höck E, Brockmann JM, Schuh WD, Krasbutter I, Kusche J, Maier A,  
4 Krauss S, Hausleitner W, Baur O, Jäggi A, Meyer U, Prange L, Pail R, Fecher T, Gruber T (2012)  
5  
6 The new combined satellite only model GOCO03s. Presented at the GGHS2012, Venice.  
7  
8  
9

10 Mecklenburg S, Drusch M, Kerr YH, Font J, Martin-Neira M, Delwart S, Buenadicha G, Reul N,  
11 Daganzo-Eusebio E, Oliva R, Crapolicchio R (2012) ESA's Soil Moisture and Ocean Salinity  
12 Mission: Mission Performance and Operations, *Geoscience and Remote Sensing*, 50 (5), 1354-  
13 1366, doi:10.1109/TGRS.2012.2187666.  
14  
15  
16  
17

18  
19  
20 Olesen AV (2002) Improved airborne scalar gravimetry for regional gravity field mapping and  
21 geoid determination. Ph.d. dissertation, National Survey and Cadastre of Denmark Technical Report  
22 24, 123 pp.  
23  
24  
25  
26

27  
28 Pail R (2003) Local gravity field continuation for the purpose of in-orbit calibration of GOCE SGG  
29 observations. *Advances in Geosciences* 1: 11–18.  
30  
31  
32

33  
34 Pail R, Bruinsma S, Migliaccio F, Foerste C, Goiginger H, Schuh W-D, Hoeck E, Reguzzoni M,  
35 Brockmann JM, Abrikosov O, Veichert M, Fecher T, Mayrhofer R, Krasbutter I, Sanso F,  
36 Tscherning CC (2011) First GOCE gravity field models derived by three different approaches.  
37 *Journal of Geodesy*, 85: 819-843. doi: 10.1007/s00190-011-0467-x.  
38  
39  
40  
41  
42

43  
44 Riedel S, Jokat W, Steinlage D (2012) Mapping tectonic provinces with airborne gravity and radar  
45 data in Dronning Maud Land, East Antarctica, *Geophysical Journal International*, 189, 414-427.  
46  
47 doi: 10.1111/j.1365-246X.2012.05363.x  
48  
49

50  
51 Rudolph S, Kusche J, Ilk K-H (2002) Investigations on the polar gap problem in ESA's gravity field  
52 and steady-state ocean circulation Explorer mission (GOCE), *Journal of Geodynamics*, 33, 65–74.  
53  
54  
55  
56  
57  
58  
59  
60

1  
2  
3 Schwarz KP, Krynski J (1977) Improvement of the geoid in local areas by satellite gradiometry,  
4  
5 Bulletin Geodesique 51: 163-176.  
6  
7

8  
9 Šprlák M, Hamácková E, Novák P (2015) Alternative validation method of satellite gradiometric  
10 data by integral transform of satellite altimetry data. Journal of Geodesy, 89: 757-773. doi:  
11 10.1007/s00190-015-0813-5.  
12  
13  
14

15  
16 Steinhage D, Helm V, Eagles G, Skou N, Kristensen SS (2013) DOMECAir 2013 Data Acquisition  
17 Report, Report submitted to ESA, (dated August 30, 2013).  
18  
19

20  
21 Tscherning CC, Rapp RH (1974) Closed covariance expressions for gravity anomalies, geoid  
22 undulations and deflections of the vertical implied by degree-variance models. Rep. 208,  
23 Department of Geodetic Science, Ohio State University, Columbus.  
24  
25  
26

27  
28 Tscherning CC, Forsberg R, Knudsen P (1992) The GRAVSOFTE package for geoid determination.  
29 Proc. IAG first continental workshop for the geoid in Europe, Prague, pp. 327-334.  
30  
31  
32

33  
34 Tscherning CC (1993) Computation of covariances of derivatives of the anomalous gravity  
35 potential in a rotated reference frame. Manuscripta Geodetica, vol. 18, 115-123, 1993.  
36  
37  
38

39  
40 Tscherning CC, Forsberg R, Albertella A, Migliaccio F, Sanso F (2000) The polar gap problem:  
41 space-wise approaches to gravity field determination in polar areas. In: Sünkel H (Ed.) From Eötvös  
42 to mGal, Final Report, ESA/ESTEC, 331-336.  
43  
44  
45  
46

47  
48 Tóth G, Rózsa S, Ádám J, Tziavos IN (2002) Gravity field modeling by torsion balance data - a  
49 case study in Hungary. In: Ádám J, Schwarz KP (Eds.) Vistas for Geodesy in the New Millennium,  
50 IAG Symposia, Vol. 125, Springer-Verlag, Berlin, Germany, pp. 193-198.  
51  
52  
53  
54  
55  
56  
57  
58  
59  
60

1  
2  
3 Tóth G, Ádám J, Földvály L, Tziavos IN, Denker H (2005) Calibration/validation of GOCE data by  
4 terrestrial torsion balance observations. In: Sansó F (Ed.) A Window on the Future Geodesy, IAG  
5 Symposia Series, 128, 214–219, Springer.  
6  
7  
8

9  
10 van Gelderen M, Rummel R (2001) The solution of the general geodetic boundary value problem  
11 by least squares. Journal of Geodesy 75: 1-11.  
12  
13  
14

15  
16 Visser P, Koop R, Klees R (2000) Scientific data production quality assessment. In: Sünkel H (Ed.)  
17 From Eötvös to mGal, Final Report, ESA/ESTEC, 157–176.  
18  
19

20  
21 Wolf KI, Denker H (2005) Upward continuation of ground data for GOCE calibration. In: Jekeli C,  
22 Bastos L, Fernandes L (eds) Gravity, Geoid and Space Missions, IAG Symposia Series, vol. 129,  
23 Springer, 60–65.  
24  
25  
26  
27

28  
29 Yildiz H (2012) A study of regional gravity field recovery from GOCE vertical gravity gradient  
30 data in the Auvergne test area using collocation. Studia Geophysica et Geodaetica 56: 171-184.  
31  
32  
33

34  
35 Zielinsky JB, Petrovskaya MS (2003) The possibility of the calibration/validation of the GOCE data  
36 with the balloon-borne gradiometer. Advances in Geosciences 1: 149–153.  
37  
38  
39  
40  
41  
42  
43  
44  
45  
46  
47  
48  
49  
50  
51  
52  
53  
54  
55  
56  
57  
58  
59  
60

## Figure Captions

**Figure 1.** The location of the Dome-C airborne gravity survey. Flight tracks are indicated by the yellow lines. The red line indicates the ferry flight from Neumayer to Dome-C.

**Figure 2.** Dome-C gravity disturbances (colour-coded), on top of flight lines (black). Units: mGal.

**Figure 3.** (a) Cross-over errors in the free-air gravity anomalies of Dome-C (b) the histogram of the absolute value of the track misties (green are “good” and yellow “bad” cross-overs relative to 10 mGal). The estimated r.m.s. error of the airborne gravity survey, based on the cross-over analysis, is 8.0 mGal.

**Figure 4.** Airborne free-air gravity anomalies and free-air gravity anomalies calculated from GOCE Direct RL4 direct global geopotential model up to spherical degree and order 200. Color scale is in mGal.

**Figure 5.** The empirical covariance function (blue) derived from the airborne gravity data, and the corresponding fitted analytical Tscherning-Rapp covariance model (red). This is typical for a good fit.

**Figure 6a.** Gradient anomalies in GRF transformed from predicted gradient anomalies in the local North-East-Up reference frame, minus ITG-GRACE10S to degree 90, for ascending tracks (left) and descending tracks (right) (a)  $T_{XX}$  (b)  $T_{XZ}$  (c)  $T_{YY}$ . Colour scale -0.04 to 0.04 Eötvös.

**Figure 6b.** Vertical gravity gradient anomalies in GRF transformed from predicted gradient anomalies in the local North-East-Up reference frame, minus ITG-GRACE10S to degree 90,  $T_{ZZ}$ . Colour scale -0.04 to 0.04 Eötvös.

**Figure 7a.** Differences between GOCE gradient anomalies in GRF and predicted gradient anomalies in GRF for ascending tracks (a)  $T_{XX}$  (b)  $T_{XZ}$  (c)  $T_{YY}$  (d)  $T_{ZZ}$ . Colour scale is -0.04 to 0.04 Eötvös. Gradient anomalies are predicted in the local North-East-Up reference frame and transformed to gradients in GRF.

**Figure 7b.** Differences between GOCE gradient anomalies in GRF and predicted gradient anomalies in GRF for descending tracks (a)  $T_{XX}$  (b)  $T_{XZ}$  (c)  $T_{YY}$  (d)  $T_{ZZ}$ . Colour scale is -0.04 to 0.04 Eötvös. Gradient anomalies are predicted in the local reference North-East-Up frame and transformed to gradient anomalies in GRF.

Figures

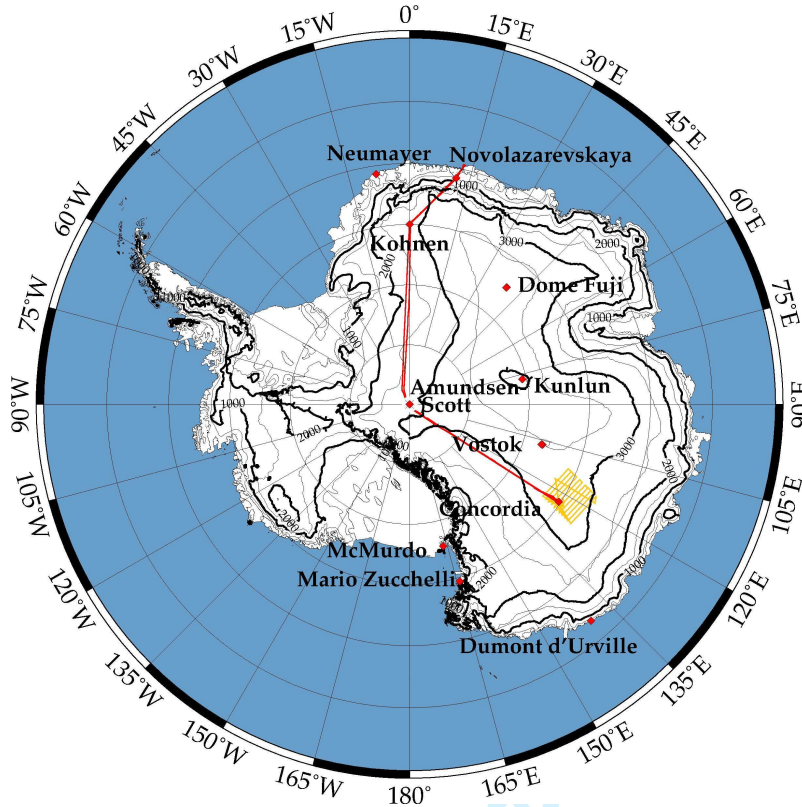
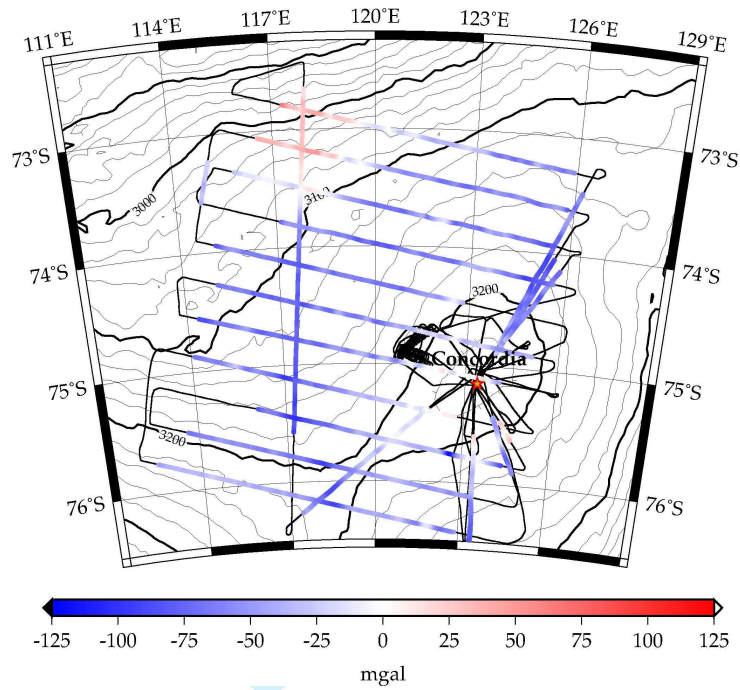
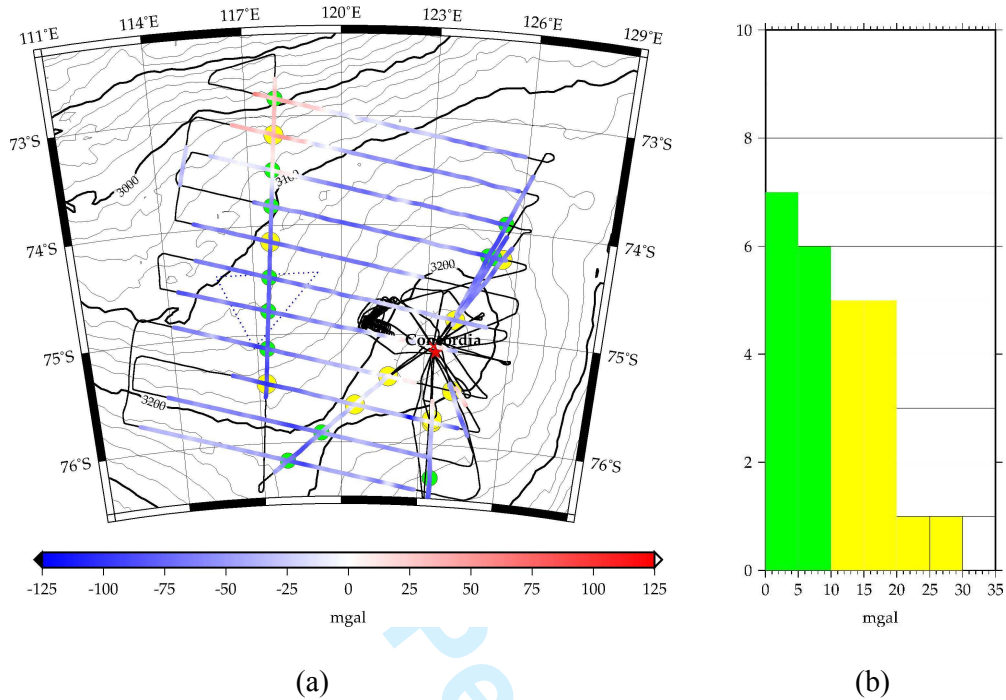


Figure 1. The location of the Dome-C airborne gravity survey. Flight tracks are indicated by the yellow lines. The red line indicates the ferry flight from Novolazarevskaya.



**Figure 2.** Dome-C gravity disturbances (colour-coded), on top of flight lines (black). Units: mGal.



**Figure 3.** (a) Cross-over errors in the free-air gravity anomalies of Dome-C (b) the histogram of the absolute value of the track misties (green are “good” and yellow “bad” cross-overs relative to 10 mgal). The estimated r.m.s. error of the AWI-processed airborne gravity survey, based on the cross-over analysis, is 8.0 mGal.



1  
2  
3  
4  
5  
6  
7  
8  
9  
10  
11  
12  
13  
14  
15  
16  
17  
18  
19  
20  
21  
22  
23  
24  
25  
26  
27  
28  
29  
30  
31  
32  
33  
34  
35  
36  
37  
38  
39  
40  
41  
42  
43  
44  
45  
46  
47  
48  
49  
50  
51  
52  
53  
54  
55  
56  
57  
58  
59  
60

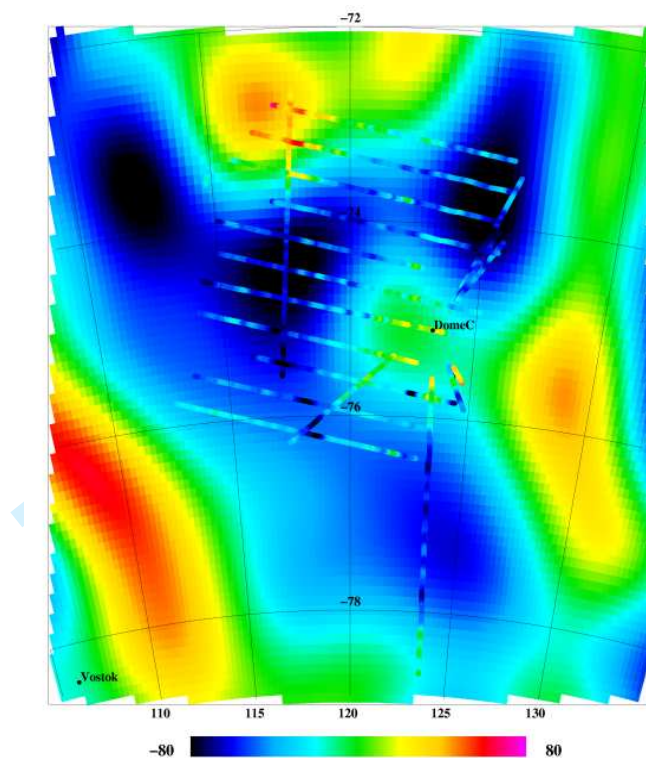


**Figure 4.** Airborne free-air gravity anomalies and free-air gravity anomalies calculated from GOCE Direct RL4 direct global geopotential model up to spherical degree and order 200. Color scale is in mGal.

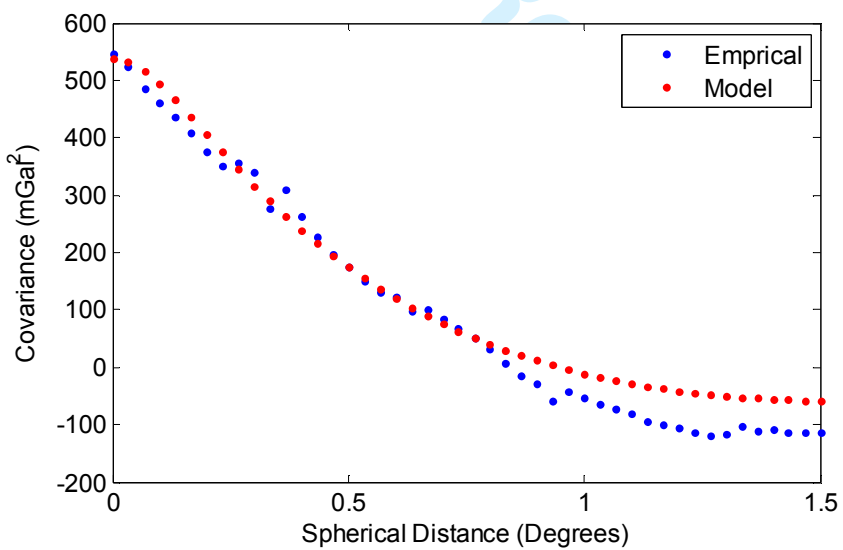


**Figure 5.** The empirical covariance function (blue) derived from the airborne gravity data, and the corresponding fitted analytical Tscherning-Rapp covariance model (red). This is typical for a good fit.



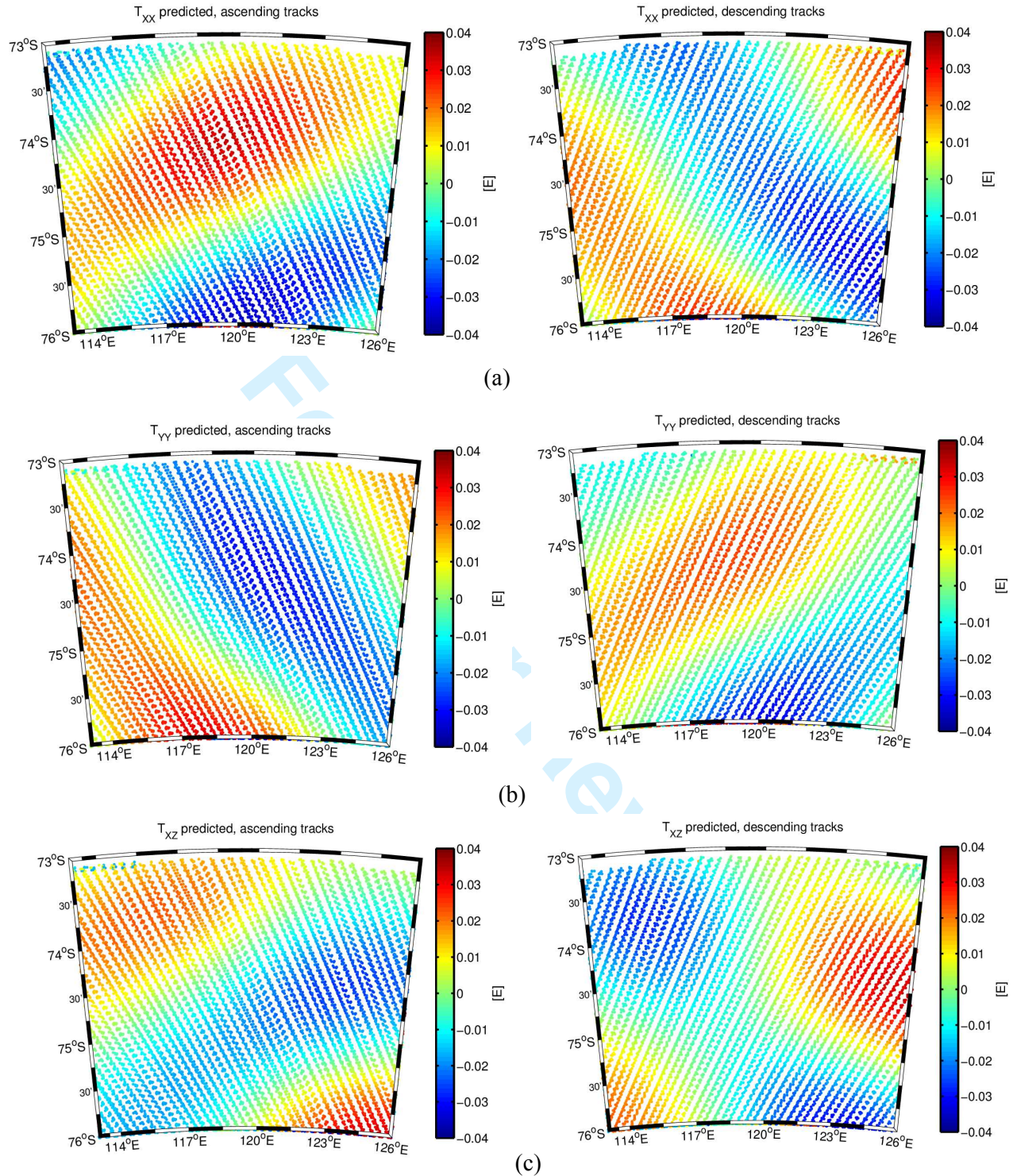


**Figure 6a.** Gradient anomalies in GRF transformed from predicted gradient anomalies in the local North-East-Up reference frame, minus ITG-GRACE10S to degree 90, for ascending tracks (left) and descending tracks (right) (a)  $T_{xx}$  (b)  $T_{xz}$  (c)  $T_{yy}$ . Colour scale -0.04 to 0.04 Eötvös.

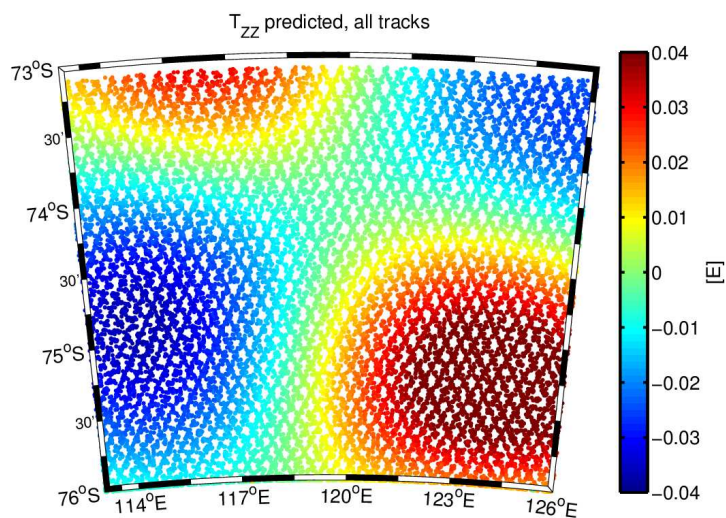


**Figure 6b.** Vertical gravity gradient anomalies in GRF transformed from predicted gradient anomalies in the local North-East-Up reference frame, minus ITG-GRACE10S to degree 90,  $T_{ZZ}$ . Colour scale -0.04 to 0.04 Eötvös.



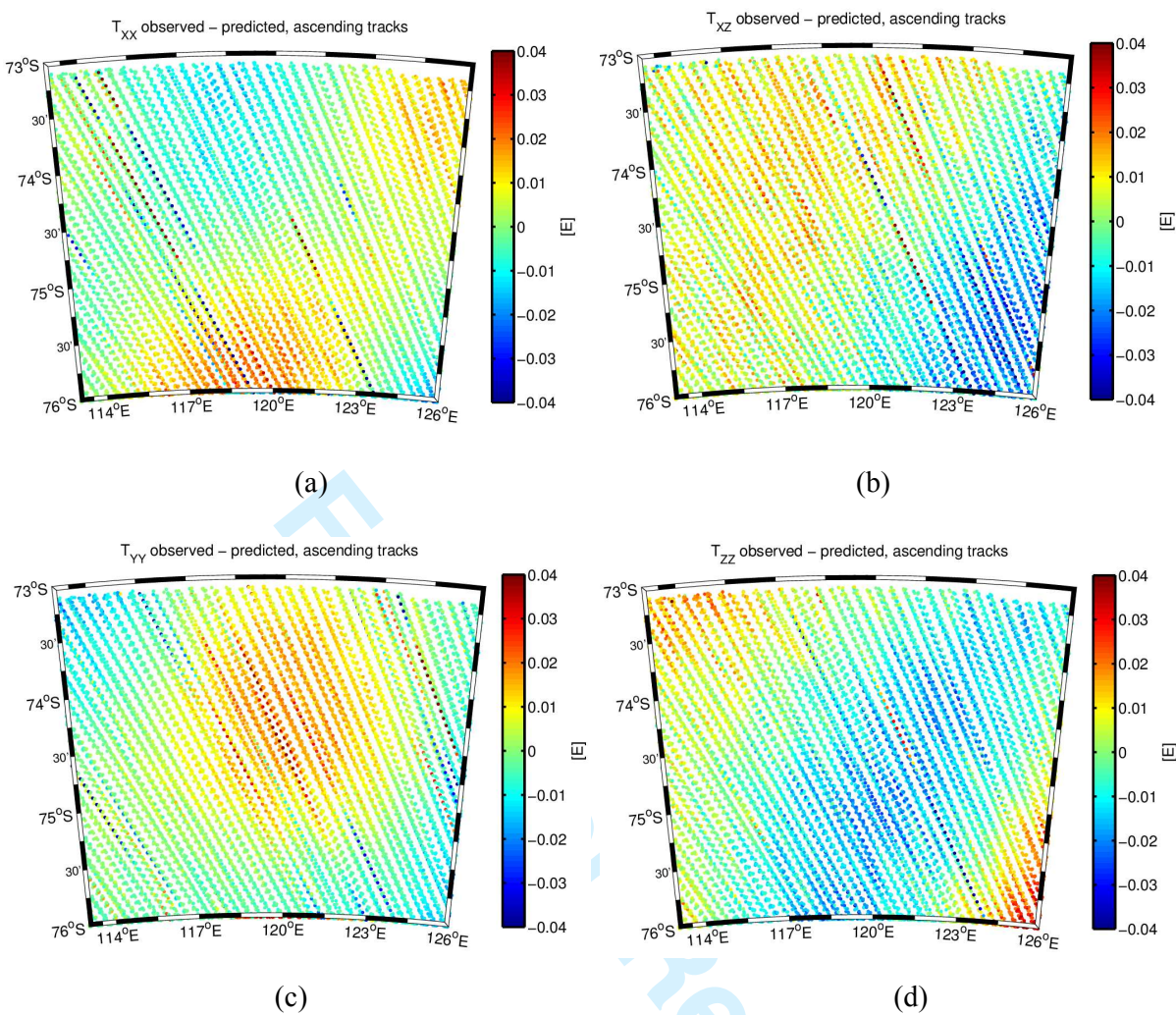


**Figure 7a.** Differences between GOCE gradient anomalies in GRF and predicted gradient anomalies in GRF for ascending tracks (a)  $T_{XX}$  (b)  $T_{XZ}$  (c)  $T_{YY}$  (d)  $T_{ZZ}$ . Colour scale is -0.04 to 0.04 Eötvös. Gradient anomalies are predicted in the local North-East-Up reference frame and transformed to gradients in GRF.

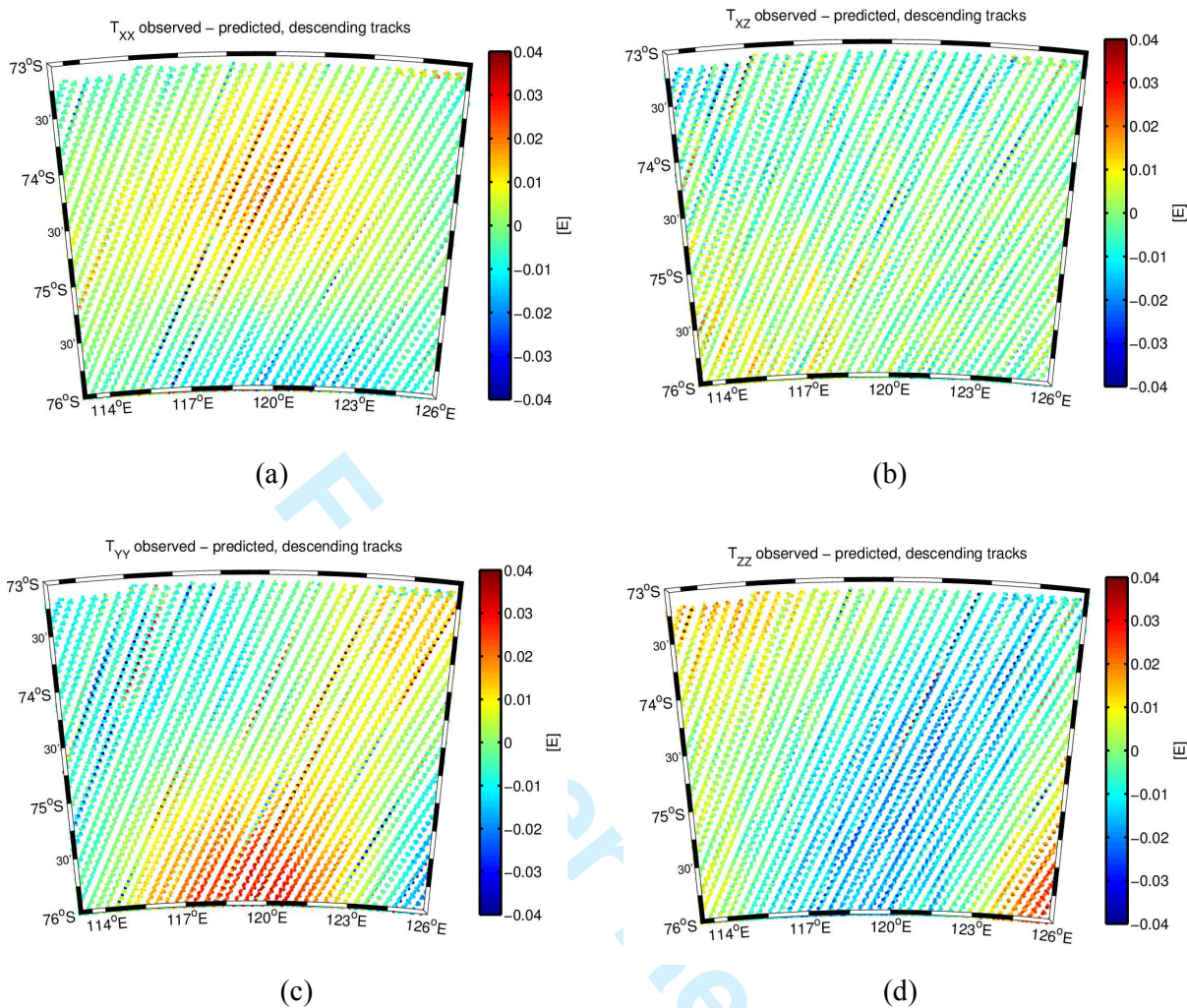


**Figure 7b.** Differences between GOCE gradient anomalies in GRF and predicted gradient anomalies in GRF for descending tracks (a)  $T_{xx}$  (b)  $T_{xz}$  (c)  $T_{yy}$  (d)  $T_{zz}$ . Colour scale is -0.04 to 0.04 Eötvös. Gradient anomalies are predicted in the local North-East-Up reference frame and transformed to gradient anomalies in GRF.

## Tables

**Table 1.** Comparison of Dome-C airborne free air gravity anomaly data to GOCE RL4 expansion (Unit is mGal).

Data for statistics	Max.	Min.	Mean	Std.dev.
Observed airborne data (51303 points)	67.9	-116.0	-40.7	28.9
Observed minus ITG-GRACE2010S to degree 90	73.9	-77.9	-2.6	24.9
Observed minus GOCE direct (max degree 120)	64.1	-87.6	0.9	22.3
- direct (max degree 180)	52.4	-93.4	0.7	18.1
- direct (max degree 200)	58.1	-91.7	2.4	16.3
- direct (max degree 220)	62.5	-97.4	1.5	15.0
- direct (max degree 250)	60.6	-96.9	1.1	14.4
- direct (max degree 260)	55.0	-91.9	0.9	16.3
Observed minus GOCE timewise (max deg 120)	64.6	-86.5	0.9	22.6
- timewise (max deg 180)	52.5	-93.1	0.7	18.1
- timewise (max deg 200)	57.5	-91.2	2.4	16.2
- timewise (max deg 220)	63.7	-95.9	1.4	14.9
- timewise (max deg 250)	62.2	-96.3	0.5	14.6

**Table 2.** Statistics of collocation upward continuation comparisons of GOCE gravity gradient (GG) anomalies in the GRF (unit: milliEötvös [mE]).

Data statistics	Txx	Txz	Tyy	Tzz
GOCE GG – GOCO03S (degree 90)				
mean	1.5	-3.0	1.7	-3.4
std.dev.	17.0	19.0	16.0	26.0
max.	106.6	93.7	102.6	111.2
min.	-113.7	-87.1	-73.6	-110.1
GOCE GG – predictions				
mean	1.9	-0.6	2.4	-4.5
std.dev.	9.9	10.4	11.5	11.6
max.	88.9	111.8	102.3	92.5
min.	-90.1	-72.7	-72.0	-91.9
Predicted error (mean) by collocation in the North-East-Up reference frame	5.8	6.7	5.5	7.9